Sensitivity Analysis of Hardfill Dams to Seismic Loading and Foundation Bearing Capacity

Anderssen Barbosa dos Santos *

Posted Date: 23 March 2026

doi: 10.20944/preprints202603.1797.v1

Keywords: hardfill dam; CSG dam; parametric analysis; seismic loading; foundation bearing capacity; finite element method

 doi:10.20944/preprints202603.1797.v1

Article

Sensitivity Analysis of Hardfill Dams to Seismic Loading and Foundation Bearing Capacity

Anderssen Barbosa dos Santos

Department of Civil Engineering and Building Engineering, University of Sherbrooke; 2500, Boulevard de l'Université, Sherbrooke, QC, J1K 2R1, Canada; anderssen.barbosa.dos.santos@usherbrooke.ca

Abstract

Hardfill dams represent a recent and cost-effective construction method in which locally available materials such as alluvial deposits, riverbed gravel, and excavation spoil are mixed with a low cement content to form the dam body. Compared with conventional roller-compacted concrete (RCC) gravity dams, hardfill dams require less rigorous material specifications and quality control, resulting in lower stresses within both the dam body and its foundation. Their symmetrical trapezoidal cross-section also provides favorable seismic performance. This paper presents a parametric sensitivity analysis of a 30 m high hardfill dam, examining the combined influence of horizontal seismic acceleration (0.1 g, 0.2 g, and 0.3 g) and foundation allowable bearing capacity (0.4, 0.6, and 0.8 MPa) on the required upstream and downstream slope inclinations. Nine models were first pre-dimensioned through rigid-body stability analysis following USACE criteria and then verified using plane-strain finite element models in SAP2000, with pseudo-static seismic loading. Results show that foundation bearing capacity is the governing parameter for the dam geometry, while seismic acceleration produces a proportional but less dominant effect on slope steepness. Gentler slopes consistently yield better stress distributions along the foundation, and significant discrepancies between rigid-body and elastic analyses arise when the foundation-to-dam stiffness ratio is low.

Keywords: hardfill dam; CSG dam; parametric analysis; seismic loading; foundation bearing capacity; finite element method

1. Introduction

The hardfill dam, also known as the cemented sand and gravel (CSG) dam, is a relatively recent type of hydraulic structure that occupies an intermediate position between conventional concrete gravity dams and earthfill embankments. The concept was first proposed by Raphael (1970) and later refined by Londe and Lino (1992), who introduced the Faced Symmetrical Hardfill Dam (FSHD) as a new alternative to roller-compacted concrete (RCC) structures. The underlying idea is to design a symmetrical trapezoidal cross-section that operates at low stress levels, thereby relaxing the strength requirements for both the dam body material and the foundation (ICOLD, 2000).

Hardfill is produced by adding a low content of cementitious material and water to rock-based aggregates such as riverbed gravel, alluvial deposits, or excavation spoil, and mixing them with simple equipment (Fujisawa et al., 2004). Because the material does not require processed aggregates or strict grading specifications, the need for quarry operations, aggregate processing plants, and turbid water treatment facilities is greatly reduced (Londe and Lino, 1992). The cement content of hardfill materials is generally no more than 90 kg/m^3 (Wu et al., 2011). Consequently, construction costs can be significantly lower than those of conventional RCC gravity dams (ICOLD, 2000).

From a mechanical standpoint, the behavior of hardfill falls in an intermediate area between concrete and rockfill materials. Before hardening, its properties resemble those of compacted rockfill; after curing, the strength and stiffness increase substantially due to cementation between grains, although they remain well below those of conventional concrete (Wu et al., 2011). The stress-strain

 doi:10.20944/preprints202603.1797.v1

behavior exhibits both frictional and cohesive mechanisms, and the material can be characterized as a cohesive-frictional medium with age-dependent properties (Wu et al., 2011; Kim et al., 2023).

From a structural dynamics perspective, the symmetrical trapezoidal cross-section of hardfill dams provides superior seismic performance compared with conventional gravity dams. In gravity dams, stress concentrations during earthquakes typically develop at the upstream heel, the downstream toe, and the change-of-slope region, threatening the structural integrity. By contrast, hardfill dams distribute stresses more uniformly over a wider foundation footprint, reducing peak stresses and improving overall dynamic stability (Xiong et al., 2013; He et al., 2025). Numerical studies have confirmed that hardfill dams remain at low stress levels and are either undamaged or only slightly damaged under moderate earthquake intensities, and that tensile cracking under overload conditions tends to occur at the upstream face rather than leading to catastrophic failure (Xiong et al., 2013; Chen et al., 2020).

In the past two decades, more than ten FSHDs have been constructed or are under construction worldwide, with heights ranging from 30 m to 107 m, the latter being the Cindere Dam in Turkey (Wu et al., 2011). In addition, temporary hardfill structures such as cofferdams and check dams have been widely adopted due to their rapid construction and overtopping capability (Wu et al., 2011; ICOLD, 2000). The favorable conditions for choosing a hardfill dam can be summarized as follows: availability of low-quality aggregates near the site, foundations with low to moderate bearing capacity, and regions with significant seismic activity.

Despite the growing number of built examples, the interplay between seismic loading intensity and foundation bearing capacity in governing the required geometry of hardfill dams has not been systematically investigated through parametric studies. Omran and Tokmechi (2010) performed a sensitivity analysis focused on geometric and material properties of symmetrical hardfill dams, while Cai et al. (2011) optimized CSG dam cross-sections using multi-objective methods. However, a combined parametric assessment that simultaneously varies seismic acceleration levels and foundation strength constraints to determine the resulting slope geometry is still lacking.

This paper addresses this gap by performing a sensitivity analysis of a 30 m high hardfill dam, systematically varying the horizontal seismic acceleration coefficient (0.1 g, 0.2 g, and 0.3 g) and the foundation allowable compressive stress (0.4, 0.6, and 0.8 MPa). For each of the nine resulting combinations, the upstream and downstream slope inclinations are first determined through rigid-body stability analysis following USACE criteria (USACE, 2005), and the resulting geometries are then verified using two-dimensional finite element models under plane-strain conditions with pseudo-static seismic loading.

2. Methodology

The analysis was conducted in two stages. In the first stage, a rigid-body equilibrium analysis was used to pre-dimension the symmetric upstream and downstream slopes of the dam for each combination of seismic acceleration and foundation bearing capacity. In the second stage, two-dimensional finite element models were constructed to verify the stress distribution along the foundation contact under elastic conditions. Both stages employed pseudo-static seismic loading.

2.1. Dam Geometry and Material Properties

The reference dam has a symmetrical trapezoidal cross-section with a crest width of 6.0 m at elevation 30.00 m and a foundation contact at elevation 0.00 m, yielding a structural height of 30 m. The upstream water level was set at elevation 29.00 m and the downstream side was considered dry. The upstream and downstream slopes were varied parametrically to satisfy the stability criteria for each loading scenario. Figure 1 illustrates the general dam cross-section.

The hardfill material properties adopted in this study are representative values drawn from the literature (Wu et al., 2011; Kim et al., 2023; Fujisawa et al., 2004). Table 1 summarizes the material parameters.

 doi:10.20944/preprints202603.1797.v1

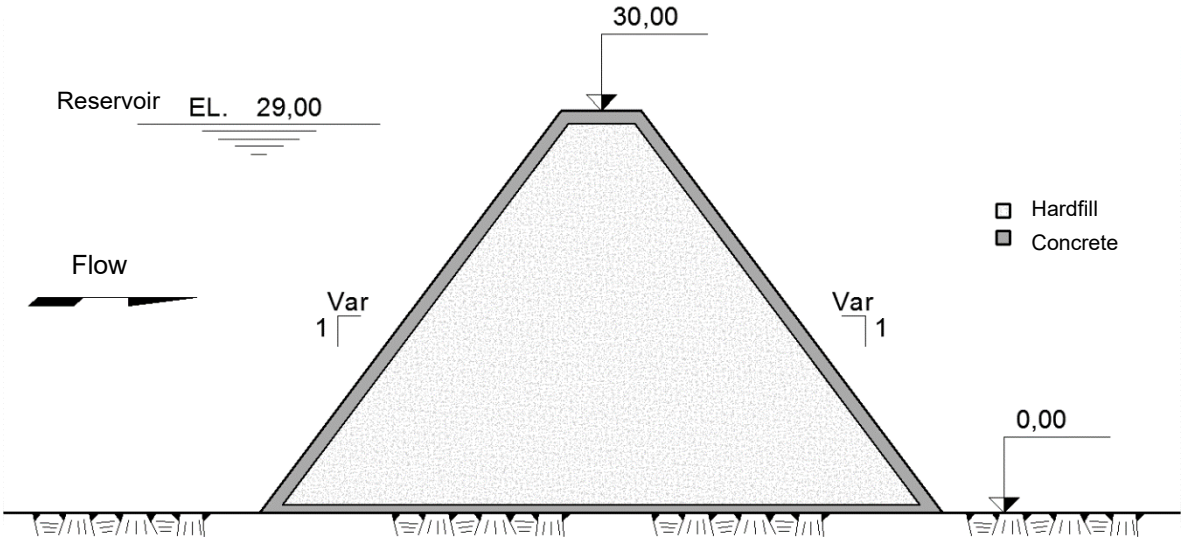

Figure 1. Typical cross-section of the hardfill dam studied.

Table 1. Hardfill material properties.

Parameter	Value
Unit weight (γ)	21.0 kN/m³
Elastic modulus (E)	12.0 GPa

2.2. Foundation Interface Parameters

The foundation was modeled as a deformable medium representative of weak rock, compacted alluvium, or cemented gravel. The concrete-to-rock interface was characterized by a cohesion of 150 kPa and a friction angle of 40°. Three levels of allowable compressive stress (0.4, 0.6, and 0.8 MPa) were considered to represent increasingly competent foundations. The foundation elastic modulus was varied as 1/10, 1/2, and 1/1 of the hardfill elastic modulus (i.e., 1.2, 6.0, and 12.0 GPa) to evaluate the effect of foundation stiffness on the stress distribution. Table 2 presents the foundation parameters.

Table 2. Foundation interface parameters.

Parameter	Value(s)
Cohesion (c)	150 kPa
Friction angle (φ)	40°
Allowable compressive stress (σf)	0.4 / 0.6 / 0.8 MPa
Elastic modulus (Ef)	1.2 / 6.0 / 12.0 GPa

2.3. Seismic Loading

Seismic effects were introduced through the pseudo-static method. Three levels of horizontal seismic acceleration were considered: a*h* = 0.1 g, 0.2 g, and 0.3 g. The vertical seismic acceleration was taken as two-thirds of the horizontal value, in accordance with USACE EM 1110-2-2100 (USACE, 2005). The hydrodynamic pressure increment due to earthquake was computed using the Westergaard added-mass approach, as prescribed in USACE EM 1110-2-2200 (USACE, 1995). Table 3 summarizes the seismic parameters.

 doi:10.20944/preprints202603.1797.v1

Table 3. Seismic loading parameters.

Parameter	Value(s)
Horizontal acceleration (ah)	0.1 / 0.2 / 0.3 g
Vertical acceleration (av = 2/3 ah)	0.067 / 0.133 / 0.200 g

2.4. Rigid-Body Stability Criteria

The rigid-body stability assessment followed the USACE criteria for concrete hydraulic structures (USACE, 2005). Three failure modes were evaluated: sliding, overturning, and base stress conditions.

Sliding stability. The factor of safety against sliding (FOS) is defined as the ratio of the resisting forces to the driving forces along the potential sliding plane: $FOS = (N \cdot \tan\varphi + c \cdot A) / T$, where N is the resultant normal force, φ is the friction angle, c is the cohesion, A is the effective contact area, and T is the resultant tangential force. The minimum required FOS values are 2.0, 1.5, and 1.1 for usual, unusual, and extreme loading conditions, respectively.

Overturning stability. Overturning was evaluated through the relative eccentricity of the resultant force with respect to the base center: $e_r = (M_R / N) / (L_{base} / 2)$. The resultant must lie within the middle third of the base for usual loads, the middle half for unusual loads, and anywhere within the base for extreme loads (USACE, 2005).

Base stress verification. For usual loading conditions, 100% of the base must remain in compression (no tensile stress allowed). For unusual conditions, at least 75% of the base must be compressed. For extreme conditions, the resultant must remain within the base. Compressive stresses must not exceed the allowable bearing capacity of the foundation.

Table 4. Required factors of safety and base compression criteria (USACE, 2005).

Criterion	Usual	Unusual	Extreme
Sliding FOS	2.0	1.5	1.1
Resultant location (er)	Middle 1/3	Middle 1/2	Within base
Base in compression	100%	75%	Resultant in base

2.5. Applied Loads

The loading scenario combined into a single extreme load case included: self-weight of the hardfill dam body, hydrostatic pressure on the upstream face, uplift pressure at the foundation contact, and pseudo-static seismic forces comprising inertial forces on the dam mass and hydrodynamic pressure computed by the Westergaard method (USACE, 1995). Figure 3 illustrates the loading scheme applied to the dam cross-section.

 doi:10.20944/preprints202603.1797.v1

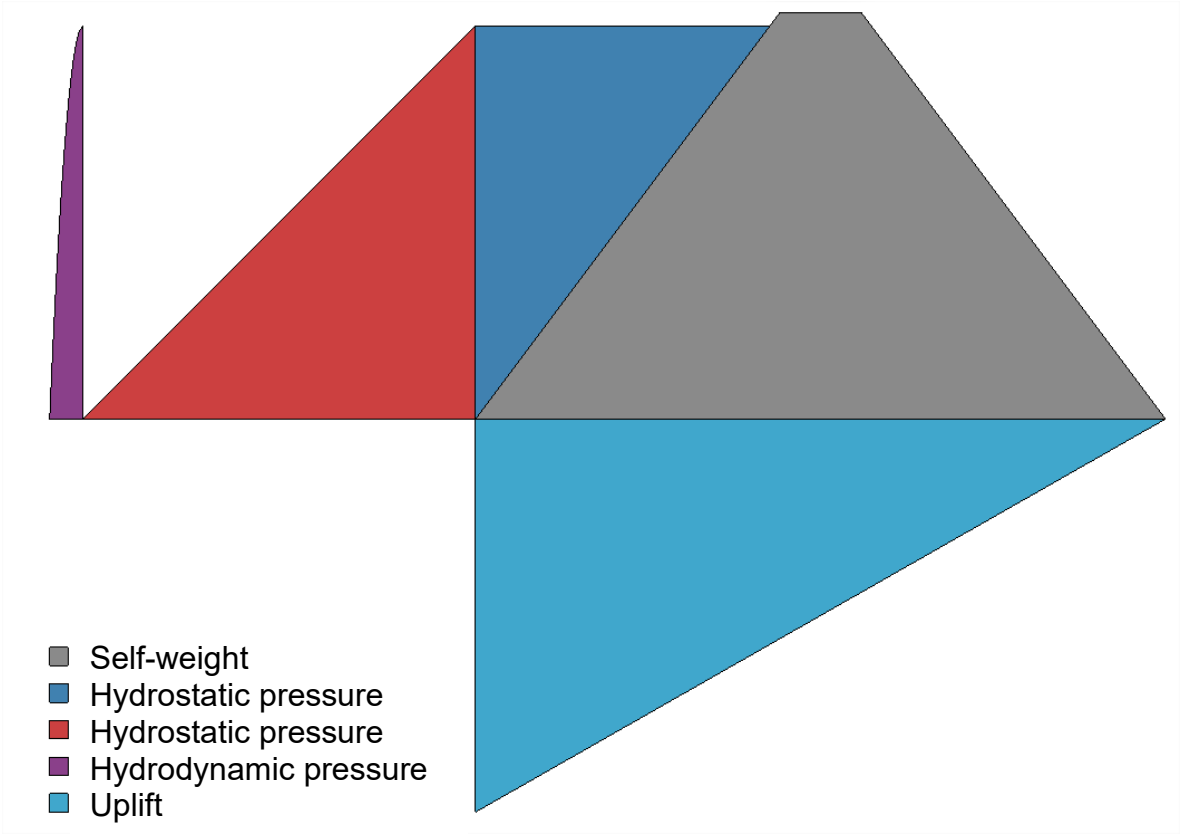

Figure 2. Applied loads on the hardfill dam cross-section.

2.6. Finite Element Model

The two-dimensional finite element analysis was carried out using SAP2000. The dam body and foundation rock were discretized with four-node quadrilateral elements under plane-strain conditions. The foundation domain extended 5 to 10 times the base width in the horizontal direction and 3 times the dam height in the vertical direction, ensuring that the boundary conditions did not influence the stress field in the region of interest.

The dam-foundation interface was modeled using nonlinear GAP link elements in the direction normal to the contact plane, allowing compression transfer only (no tensile resistance). Horizontal displacement compatibility between the dam and foundation was enforced through equal-displacement constraints, a condition justified by the prior verification that sliding stability was satisfied under the USACE criteria. Figure 4 shows a representative finite element mesh.

 doi:10.20944/preprints202603.1797.v1

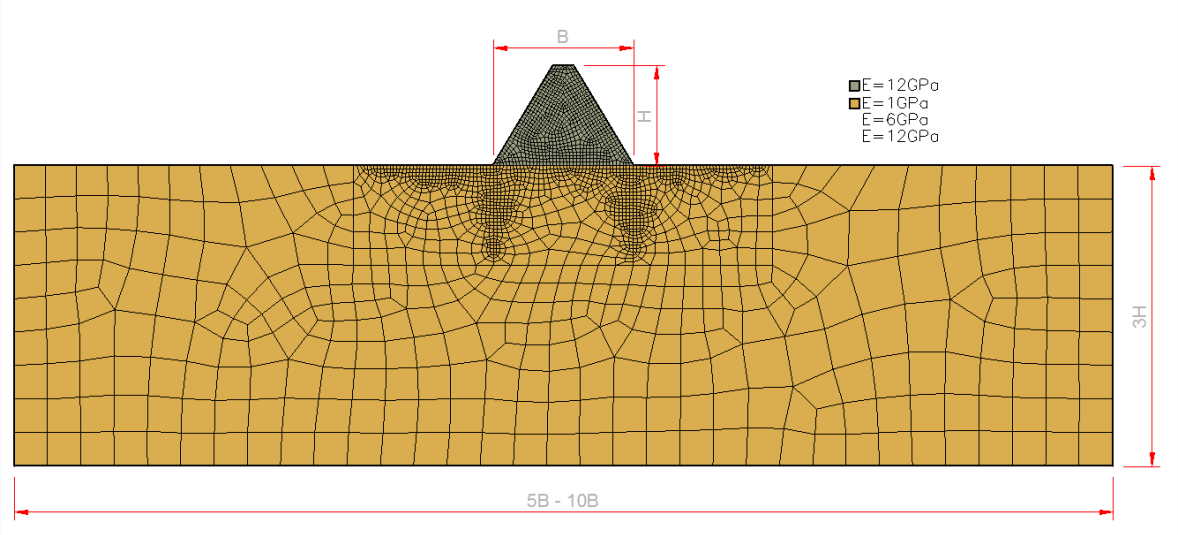

Figure 3. Two-dimensional finite element model of the hardfill dam and foundation.

3. Results and Discussion

Nine models were analyzed, corresponding to all combinations of three seismic acceleration levels (0.1 g, 0.2 g, and 0.3 g) and three foundation bearing capacities (0.4, 0.6, and 0.8 MPa). For each combination, the symmetric slope inclination was first determined from the rigid-body analysis and then the resulting geometry was verified using the finite element model. Table 5 summarizes the results of all nine models, and Figures 4 through 9 present the dam geometry and base stress distribution for each case.

Table 5. Summary of parametric analysis results.

Model	ah (g)	σf (MPa)	Slope (H:V)	Peak σ (MPa)
1	0.1	0.4	0.9:1.0	1.4
2	0.1	0.6	0.5:1.0	0.7
3	0.1	0.8	0.5:1.0	1.1
4	0.2	0.4	1.0:1.0	0.5
5	0.2	0.6	0.6:1.0	0.9
6	0.2	0.8	0.5:1.0	1.05
7	0.3	0.4	1.1:1.0	0.6
8	0.3	0.6	0.8:1.0	1.2
9	0.3	0.8	0.5:1.0	2.1

 doi:10.20944/preprints202603.1797.v1

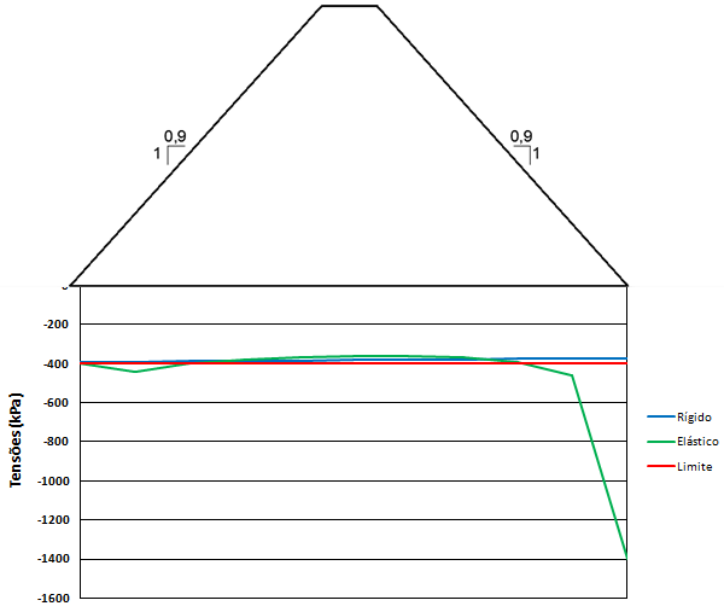

Figure 4. Model 1 (ah = 0.1 g, σf = 0.4 MPa): dam geometry and vertical stress distribution along the foundation.

3.1. Effect of Foundation Bearing Capacity on Dam Geometry

The results in Table 5 demonstrate that the foundation allowable compressive stress is the dominant parameter governing the required slope inclination. For a constant seismic acceleration of 0.1 g, reducing the bearing capacity from 0.8 MPa to 0.4 MPa required the slope to increase from 0.5H:1.0V to 0.9H:1.0V, nearly doubling the dam footprint. The same pattern is observed at higher seismic levels: at 0.3 g, the slope changes from 0.5H:1.0V to 1.1H:1.0V as the bearing capacity decreases from 0.8 MPa to 0.4 MPa. This confirms that the foundation bearing constraint is more influential on the dam geometry than the seismic loading level.

This finding is consistent with the design philosophy of hardfill dams, which are specifically intended for sites with lower-quality foundations. As noted by Londe and Lino (1992), the symmetrical section of the FSHD is designed to operate at low stress levels, making the allowable foundation pressure the critical design constraint. The results of the present study provide quantitative support for this principle.

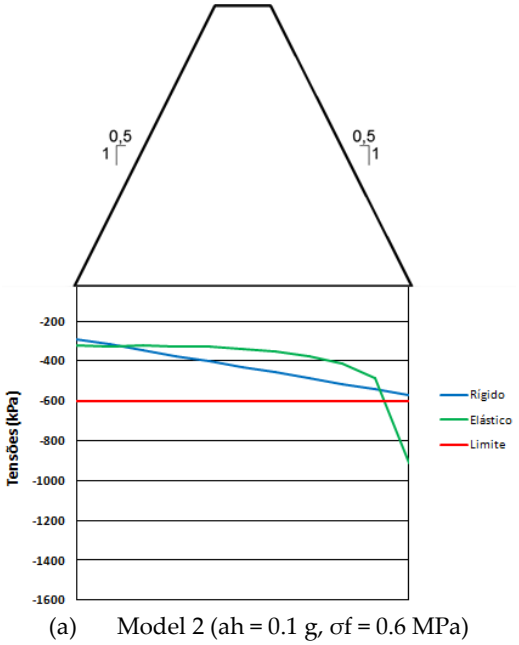

(a) Model 2 (ah = 0.1 g, σf = 0.6 MPa)

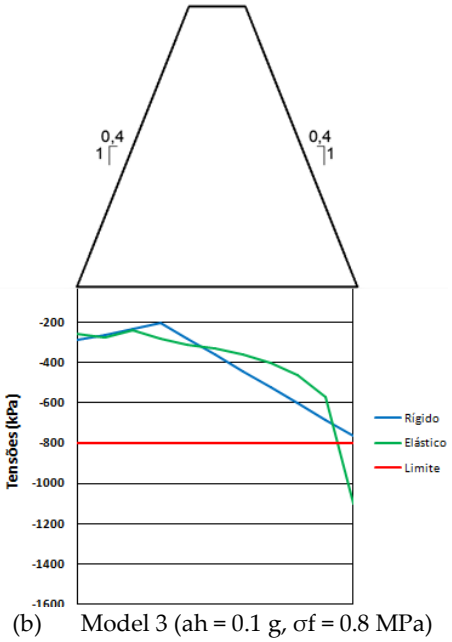

(b) Model 3 (ah = 0.1 g, σf = 0.8 MPa)

 doi:10.20944/preprints202603.1797.v1

Figure 5. Model 2 and 3: dam geometry and vertical stress distribution along the foundation.

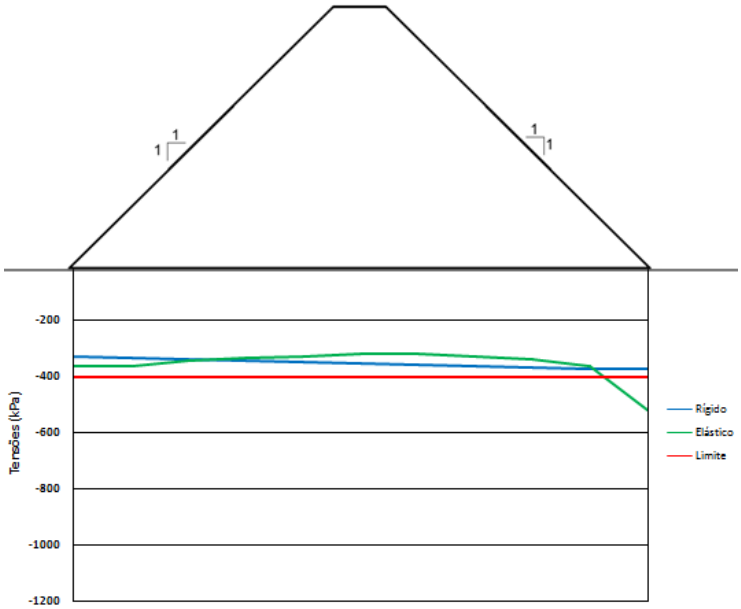

Figure 6. Model 4 (ah = 0.2 g, σf = 0.4 MPa): dam geometry and vertical stress distribution along the foundation.

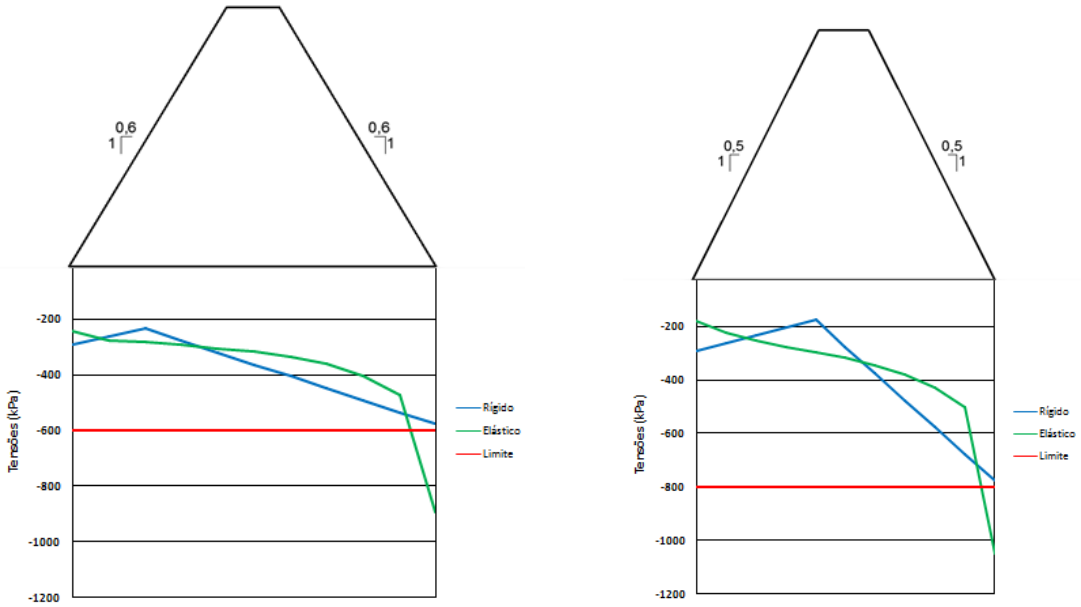

(a) Model 5 (ah = 0.2 g, σf = 0.6 MPa) (b) Model 6 (ah = 0.2 g, σf = 0.8 MPa)

Figure 7. Model 5 and 6: dam geometry and vertical stress distribution along the foundation.

 doi:10.20944/preprints202603.1797.v1

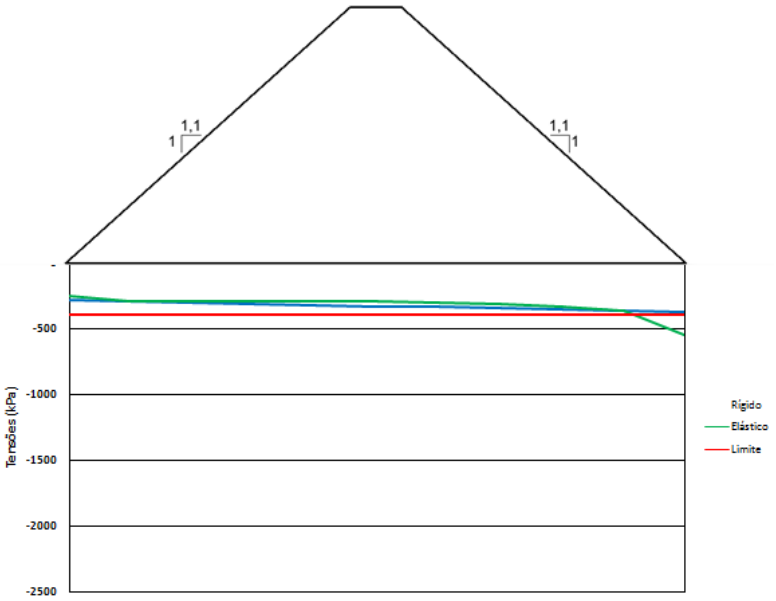

Figure 8. Model 7 (ah = 0.3 g, σf = 0.4 MPa): dam geometry and vertical stress distribution along the foundation.

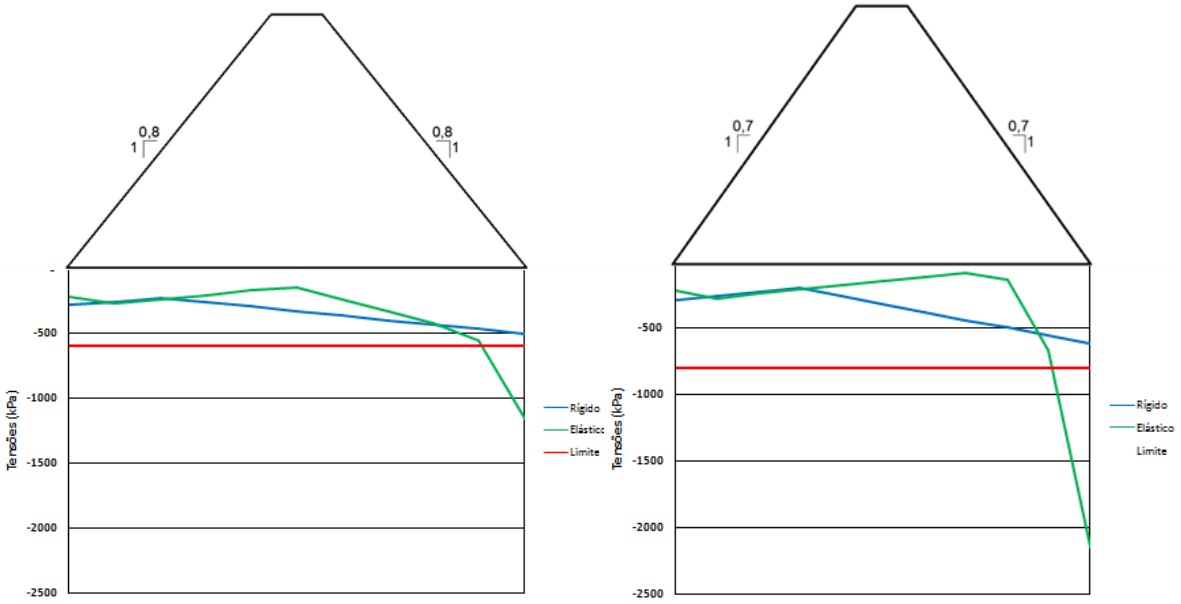

(a) Model 8 (ah = 0.3 g, σf = 0.6 MPa) (b) Model 9 (ah = 0.3 g, σf = 0.8 MPa)

Figure 9. Model 8 and 9: dam geometry and vertical stress distribution along the foundation.

3.2. Effect of Seismic Acceleration on Dam Geometry

For a given bearing capacity, increasing the seismic acceleration from 0.1 g to 0.3 g produces a proportional increase in the required slope inclination. At σ_f = 0.4 MPa, the slope increases from 0.9H:1.0V to 1.1H:1.0V as the acceleration rises from 0.1 g to 0.3 g. At σ_f = 0.6 MPa, the slope changes from 0.5H:1.0V to 0.8H:1.0V. While the effect is proportional and consistent, its magnitude is smaller than that of the bearing capacity variation, confirming that seismic loading is a secondary driver of the dam cross-section dimensions.

This favorable seismic behavior is attributed to the wide, symmetrical footprint of the hardfill dam, which distributes inertial forces over a large base area and keeps stress levels low. Xiong et al. (2013) reported similar conclusions, finding that hardfill dams maintain low stress levels and suffer only slight damage under moderate seismic intensities. He et al. (2025) further showed that the

 doi:10.20944/preprints202603.1797.v1

seismic response of hardfill dams is sensitive to the choice of earthquake input model but generally remains within acceptable limits for well-proportioned sections.

3.3. Comparison Between Rigid-Body and Finite Element Results

In all nine models, the finite element analysis revealed peak compressive stresses at the downstream toe that exceeded the values predicted by the rigid-body analysis, and in most cases also exceeded the allowable foundation bearing capacity. This stress concentration at the downstream toe is a well-known phenomenon in gravity-type dams subjected to combined static and seismic loading, and it is caused by the eccentricity of the resultant force toward the downstream side.

The discrepancy between rigid-body and elastic results was strongly influenced by the foundation-to-dam stiffness ratio. When the foundation elastic modulus was significantly lower than that of the hardfill (E_f/E_{dam} = 1/10), the stress redistribution in the elastic model was substantial, leading to peak stresses considerably higher than the uniform distribution assumed in the rigid-body approach. As the stiffness ratio increased toward unity, the elastic and rigid-body results converged, with the stress distribution becoming more uniform along the base. This observation highlights the importance of performing finite element verification when the foundation is significantly more deformable than the dam body, a condition that is common in hardfill dam applications where foundations may consist of weak rock or compacted alluvium.

3.4. Stress Distribution Patterns

Across all models, gentler slopes (larger H:V ratios) consistently produced more uniform stress distributions along the foundation, with lower peak compressive stresses. For example, Model 4 (slope 1.0H:1.0V, a_h = 0.2 g, σ_f = 0.4 MPa) exhibited a peak stress of only 0.5 MPa, while Model 9 (slope 0.5H:1.0V, a_h = 0.3 g, σ_f = 0.8 MPa) reached 2.1 MPa despite having a higher allowable bearing capacity. This confirms that the wider base associated with gentler slopes is the most effective mechanism for controlling foundation stresses in hardfill dams, and that steep slopes combined with high seismic accelerations can lead to unacceptable stress concentrations even when the foundation material itself is relatively competent.

4. Conclusions

A parametric sensitivity analysis of a 30 m high hardfill dam was performed, combining rigid-body stability assessment with plane-strain finite element verification under pseudo-static seismic loading. Nine models were analyzed, covering three levels of horizontal seismic acceleration (0.1 g, 0.2 g, 0.3 g) and three levels of foundation allowable compressive stress (0.4, 0.6, 0.8 MPa). The main conclusions are as follows:

(1) Foundation bearing capacity is the governing parameter for the determination of the hardfill dam cross-section geometry. Reducing the allowable foundation stress from 0.8 MPa to 0.4 MPa approximately doubled the required slope inclination across all seismic levels, demonstrating that the bearing constraint has a greater influence on dam dimensions than the seismic loading intensity.

(2) Increasing seismic acceleration produces a proportional but secondary increase in the required slope inclination. For a given bearing capacity, the slope increment from 0.1 g to 0.3 g was consistent but smaller in magnitude than the effect of varying the foundation strength. This confirms the favorable seismic performance of the symmetrical trapezoidal cross-section, which distributes inertial forces over a wide base.

(3) Gentler slopes yield significantly better stress distributions along the foundation. Models with wider bases exhibited lower and more uniform peak compressive stresses, while steep slopes combined with high seismic accelerations led to pronounced stress concentrations at the downstream toe.

(4) Significant discrepancies exist between rigid-body and finite element results, particularly when the foundation-to-dam stiffness ratio is low. The rigid-body approach underestimates peak

 doi:10.20944/preprints202603.1797.v1

compressive stresses because it assumes a linear stress distribution, whereas the elastic analysis captures the stress concentration at the downstream toe. This finding underscores the necessity of performing finite element verification for hardfill dams on deformable foundations.

(5) For future research, it is recommended to extend this parametric study to include variation of the interface shear parameters (cohesion and friction angle) to evaluate the influence of sliding stability on the required geometry, and to employ dynamic time-history analysis instead of the pseudo-static approach to capture frequency-dependent amplification effects. Additionally, the incorporation of material nonlinearity and damage models, such as those proposed by Wu et al. (2011) and Xiong et al. (2013), would improve the realism of the seismic performance assessment.

References

1. Cai, X., Wu, Y., Yi, J. and Ming, Y. (2011). Research on shape optimization of CSG dams. *Water Science and Engineering*, 4(4), pp. 445–454. doi:10.3882/j.issn.1674-2370.2011.04.008.
2. Chen, J., Liu, P., Xu, Q. and Li, J. (2020). Seismic analysis of hardfill dams considering spatial variability of material parameters. *Engineering Structures*, 211, 110439. doi:10.1016/j.engstruct.2020.110439.
3. Fujisawa, T., Nakamura, A., Kawasaki, H., Hirayama, D., Yamaguchi, Y. and Sasaki, T. (2004). Material properties of CSG for the seismic design of trapezoid-shaped CSG dam. In: *Proceedings of the 13th World Conference on Earthquake Engineering*, Vancouver, Canada, Paper No. 292.
4. He, W.-P., Song, J.-J., Liu, W. and Cao, X.-W. (2025). Influence of physical characteristics of earthquake input model on seismic response of hardfill dam. *Journal of Earthquake Engineering*, 29(2), pp. 308–323. doi:10.1080/13632469.2024.2443629.
5. ICOLD (2000). *The Gravity Dam: A Dam for the Future — Review and Recommendations*. Bulletin 117. Paris: International Commission on Large Dams.
6. Kim, S., Choi, W., Kim, Y., Shin, J. and Kim, B. (2023). Investigation of compressive strength characteristics of hardfill material and seismic stability of hardfill dams. *Applied Sciences*, 13(4), 2492. doi:10.3390/app13042492.
7. Londe, P. and Lino, M. (1992). The faced symmetrical hardfill dam: a new concept for RCC. *Water Power and Dam Construction*, 44(1), pp. 19–24.
8. Mason, P. J. and Molyneux, J. D. (2008). The design and construction of a faced symmetrical hardfill dam. *Hydropower and Dams*, 15(5), pp. 90–95.
9. Omran, M. E. and Tokmechi, Z. (2010). Sensitivity analysis of symmetrical hardfill dams. *Middle-East Journal of Scientific Research*, 5(6), pp. 470–477.
10. Raphael, J. M. (1970). The optimum gravity dam. In: *Rapid Construction of Concrete Dams*. ASCE, pp. 1–21.
11. USACE (1995). *Gravity Dam Design*. Engineer Manual EM 1110-2-2200. Washington, DC: U.S. Army Corps of Engineers.
12. USACE (2005). *Stability Analysis of Concrete Structures*. Engineer Manual EM 1110-2-2100. Washington, DC: U.S. Army Corps of Engineers.
13. Wu, M. X., Du, B., Yao, Y. C. and He, X. F. (2011). An experimental study on stress-strain behavior and constitutive model of hardfill material. *Science China Physics, Mechanics & Astronomy*, 54(11), pp. 2015–2024. doi:10.1007/s11433-011-4518-3.
14. Xiong, K., He, Y., Jin, F. and Liu, Y. (2013). Seismic failure modes and seismic safety of hardfill dam. *Water Science and Engineering*, 6(2), pp. 199–214. doi:10.3882/j.issn.1674-2370.2013.02.008.